nature biomedical engineering

Supplementary information

https://doi.org/10.1038/s41551-026-01765-w

Engineered lipid nanoparticles for in vivo and durable editing of haematopoietic stem cells within humanized mice

In the format provided by the authors and unedited

Supplementary Figures

Supplementary Fig. 1 Engineering of CD34-overexpressing K562 clonal cells.

(a) Schematic illustration of the lentiviral construct for CD34 overexpression. SFFV, promoter; BlastR, Blasticidin-resistant gene.

(b) Flow cytometry plots exemplifying the percentage of $CD34^+$ K562 cells. WT K562 cells were transduced with the CD34-overexpressing lentivirus at a multiplicity of infection (MOI) of 0.1. Subsequently, $CD34^+$ K562 cells were enriched by Blasticidin-based resistance selection and fluorescence-activated cell sorting (FACS).

(c) Representative flow cytometry plots showing the percentage of $CD34^+$ cells in WT K562 cells, $CD34^+$ K562 cells and primary human $CD34^+$ HSPCs.

(d-e) Quantification of the percentage of $CD34^+$ cells **(d)** and mean fluorescence intensity (MFI) of CD34 expression levels **(e)**, corresponding to panel **c**. Data are represented as mean ± s.d. (n = 3 biologically independent samples). Statistical significance was analyzed using unpaired two-sided student's *t*-test, NS, not significant.

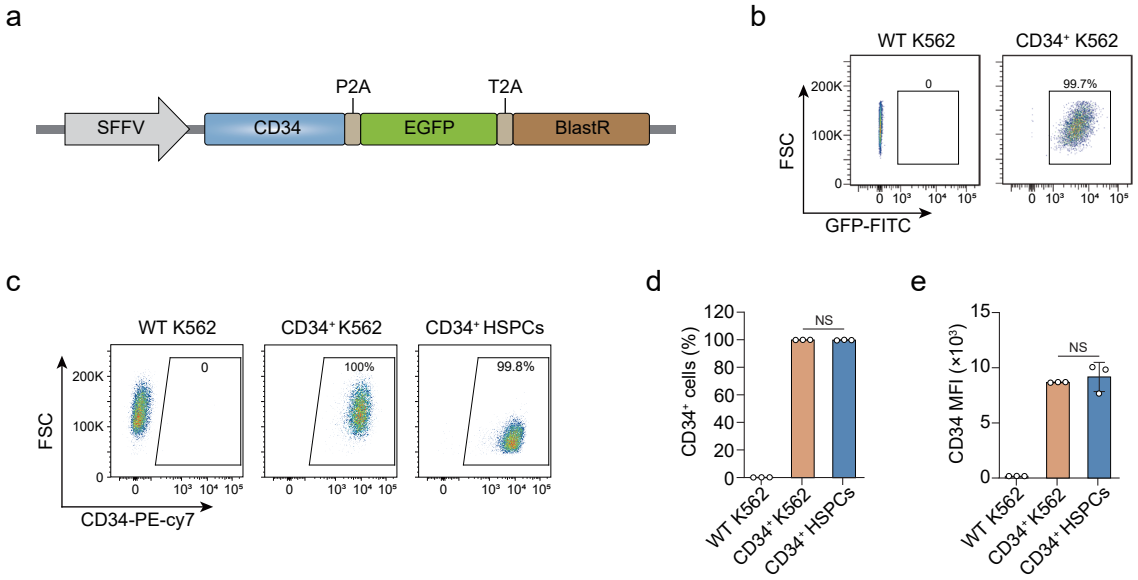
a
SFFV
CD34
P2A
EGFP
T2A
BlastR
b
WT K562
CD34⁺ K562
0
99.7%
FSC
GFP-FITC
c
WT K562
CD34⁺ K562
CD34⁺ HSPCs
0
100%
99.8%
FSC
CD34-PE-cy7
d
CD34⁺ cells (%)
NS
WT K562
CD34⁺ K562
CD34⁺ HSPCs
e
CD34 MFI (×10³)
NS
WT K562
CD34⁺ K562
CD34⁺ HSPCs

Supplementary Fig. 2 Comprehensive physicochemical characterization of CD34/LNP^{DS} engineered with diverse antibody-to-maleimide molar ratios.

(a-c) The zeta potential **(a)**, PDI **(b)** and average size **(c)** of LNP^{DS} and various CD34/LNP^{DS} formulations engineered with varying antibody-to-maleimide ratios (ranging from 0.025:1 to 0.40:1), as measured by dynamic light scattering.

(d) Encapsulation efficiency of mCherry mRNA within CD34/LNP^{DS} formulations across a spectrum of antibody-to-maleimide ratios. Ab, antibody; Mal, maleimide. Data are presented as mean ± s.d. (n = 3 biologically independent samples).

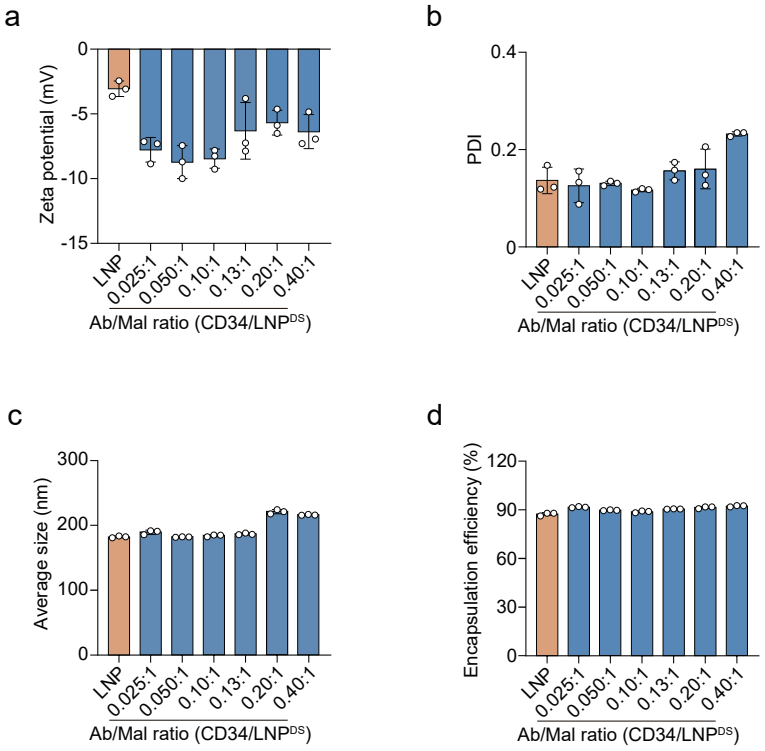
a
Zeta potential (mV)
0
-5
-10
-15
LNP
0.025:1
0.050:1
0.10:1
0.13:1
0.20:1
0.40:1
Ab/Mal ratio (CD34/LNP^DS)
b
PDI
0.4
0.2
0
LNP
0.025:1
0.050:1
0.10:1
0.13:1
0.20:1
0.40:1
Ab/Mal ratio (CD34/LNP^DS)
c
Average size (nm)
300
200
100
0
LNP
0.025:1
0.050:1
0.10:1
0.13:1
0.20:1
0.40:1
Ab/Mal ratio (CD34/LNP^DS)
d
Encapsulation efficiency (%)
120
90
60
30
0
LNP
0.025:1
0.050:1
0.10:1
0.13:1
0.20:1
0.40:1
Ab/Mal ratio (CD34/LNP^DS)

Supplementary Fig. 3 Evaluation of LNP^{DS} and CD34/LNP^{DS} transfection in WT K562 cells.

(a) Representative flow cytometry plots showing the transfection efficiency (% $mCherry^+$ cells) of LNP^{DS}-mCherry and CD34/LNP^{DS}-mCherry prepared with varying antibody-to-mal ratios, in WT K562 cells (1×10^5 cells/mL). A concentration of 500 ng/mL LNPs was utilized.

(b) Quantitative analysis of the percentage of $mCherry^+$ cells within WT K562 cells (related to panel **a**). Data are presented as mean ± s.d. (n = 3 biologically independent samples).

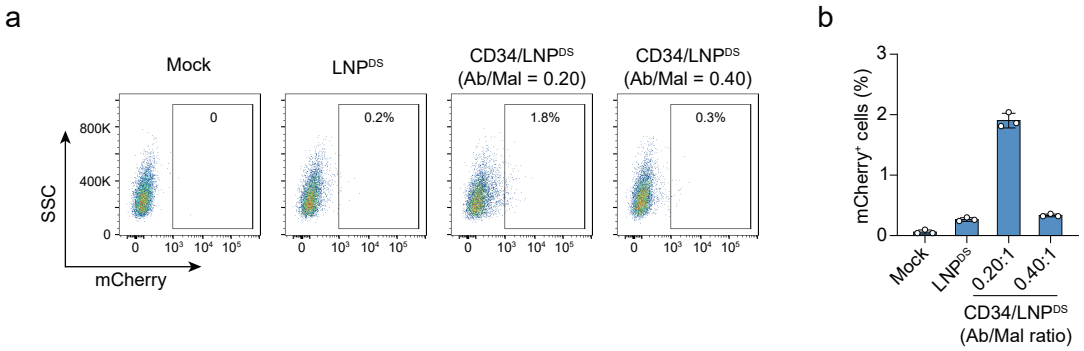
a
Mock
LNP^DS
CD34/LNP^DS (Ab/Mal = 0.20)
CD34/LNP^DS (Ab/Mal = 0.40)
0
0.2%
1.8%
0.3%
800K
400K
0
SSC
mCherry
0
10^3
10^4
10^5
b
mCherry+ cells (%)
3
2
1
0
Mock
LNP^DS
0.20:1
0.40:1
CD34/LNP^DS
(Ab/Mal ratio)

Supplementary Fig. 4 Evaluation of transfection efficiency and cell viability in $CD34^+$ K562 cells mediated by $CD34/LNP^{DS}$ delivery.

(a) Representative flow cytometry plots showing $CD34/LNP^{DS}$-mCherry transfection efficiency (% $mCherry^+$ cells) in $CD34^+$ K562 cells. Cells were plated at a density of 1×10^5 cells/mL and treated with varying concentrations of $CD34/LNP^{DS}$ ranging from 50 ng/mL to 1,000 ng/mL, followed by flow cytometric analysis.

(b) Assessment of $CD34^+$ K562 cell viability using the CellTiter-Lumi assay. Cells were incubated with LNP^{DS}, IgG/LNP^{DS} or $CD34/LNP^{DS}$ at concentrations ranging from 50 to 1,000 ng/mL for 48 hours (n = 3 biologically independent samples).

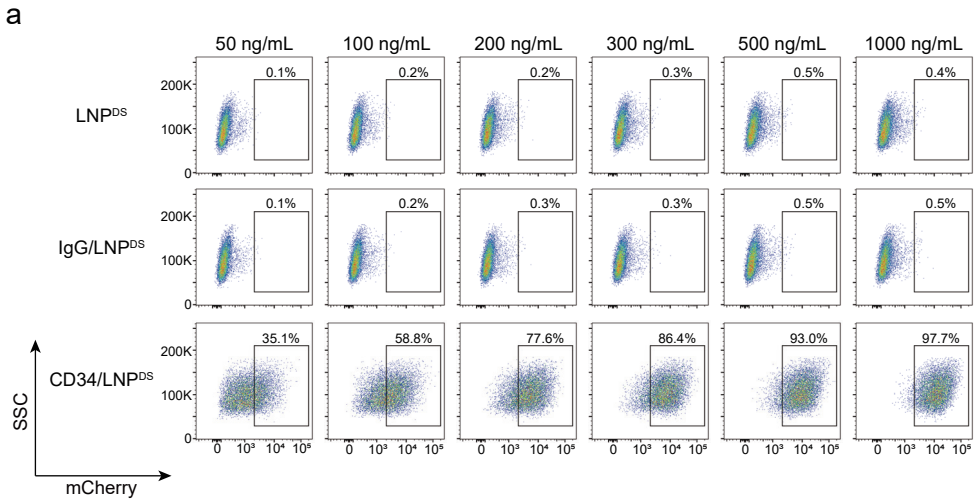
a
50 ng/mL
100 ng/mL
200 ng/mL
300 ng/mL
500 ng/mL
1000 ng/mL
LNPDS
IgG/LNPDS
CD34/LNPDS
0.1%
0.2%
0.2%
0.3%
0.5%
0.4%
0.1%
0.2%
0.3%
0.3%
0.5%
0.5%
35.1%
58.8%
77.6%
86.4%
93.0%
97.7%
200K
100K
0
SSC
mCherry

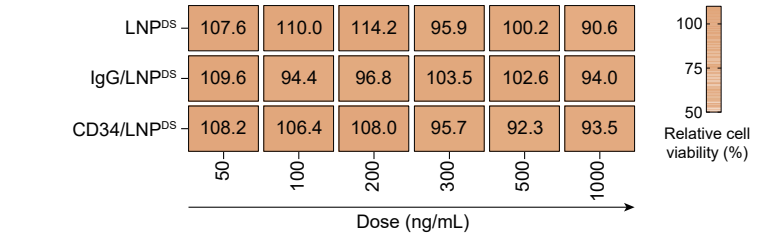
b
LNPDS
IgG/LNPDS
CD34/LNPDS
107.6
110.0
114.2
95.9
100.2
90.6
109.6
94.4
96.8
103.5
102.6
94.0
108.2
106.4
108.0
95.7
92.3
93.5
50
100
200
300
500
1000
Dose (ng/mL)
100
75
50
Relative cell viability (%)

Supplementary Fig. 5 Evaluation of transfection efficiency and cell viability in WT K562 cells mediated by CD34/LNP^{DS} delivery.

(a) Representative flow cytometry plots showing CD34/LNP^{DS}-mCherry transfection efficiency (% mCherry^{+} cells) in WT K562 cells. Cells were plated at a density of 1 × 10^{5} cells/mL and treated with varying concentrations of LNP^{DS}, IgG/LNP^{DS} or CD34/LNP^{DS} ranging from 50 ng/mL to 1,000 ng/mL, followed by flow cytometric analysis.

(b) Assessment of WT K562 cell viability using the CellTiter-Lumi assay. Cells were incubated with LNP^{DS}, IgG/LNP^{DS} or CD34/LNP^{DS} at concentrations ranging from 50 to 1,000 ng/mL for 48 hours (n = 3 biologically independent samples).

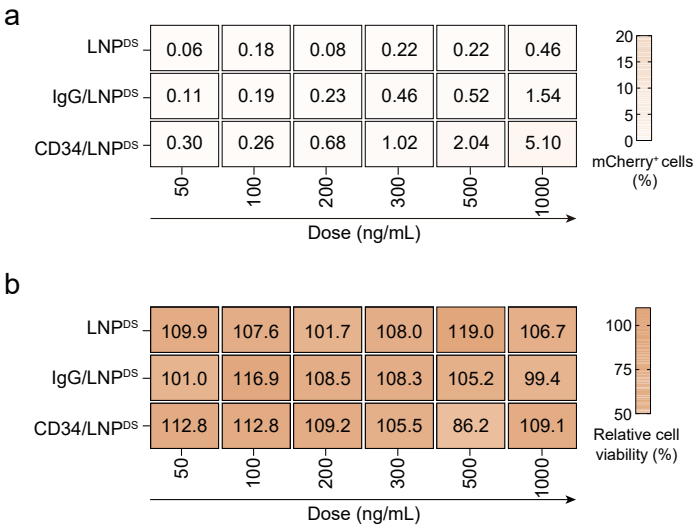
a
LNP^DS
IgG/LNP^DS
CD34/LNP^DS
0.06
0.18
0.08
0.22
0.22
0.46
0.11
0.19
0.23
0.46
0.52
1.54
0.30
0.26
0.68
1.02
2.04
5.10
50
100
200
300
500
1000
Dose (ng/mL)
20
15
10
5
0
mCherry+ cells (%)
b
LNP^DS
IgG/LNP^DS
CD34/LNP^DS
109.9
107.6
101.7
108.0
119.0
106.7
101.0
116.9
108.5
108.3
105.2
99.4
112.8
112.8
109.2
105.5
86.2
109.1
50
100
200
300
500
1000
Dose (ng/mL)
100
75
50
Relative cell viability (%)

Supplementary Fig. 6 Assessment of the physicochemical characteristics and transfection efficacy of CD34/LNP^{DS} following prolonged storage.

(a) CD34/LNP^{DS} (Ab/Mal = 0.20) were formulated and stored at 4 °C. Over a period of 15 days, the dynamic light scattering technique was employed to monitor the temporal variations in both the average size and PDI of the CD34/LNP^{DS} formulations.

(b) The transfection efficiency of CD34/LNP^{DS} was evaluated following a 48-hour co-incubation with CD34^{+} K562 cells. A concentration of 500 ng/mL CD34/LNP^{DS} was administered. Data are presented as mean ± s.d. (n=3 biologically independent samples).

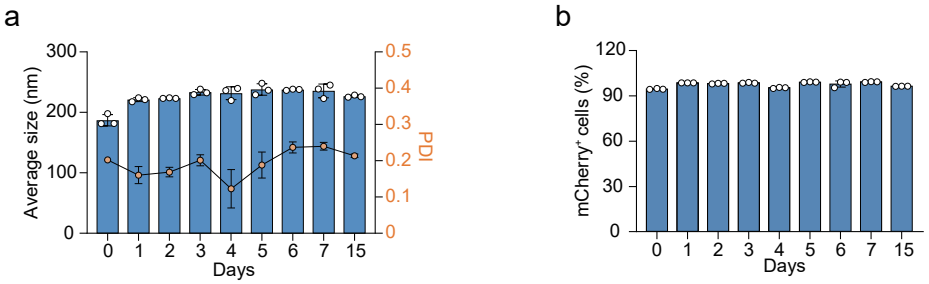
a
Average size (nm)
300
200
100
0
0.5
0.4
0.3
0.2
0.1
0
PDI
0 1 2 3 4 5 6 7 15
Days
b
mCherry+ cells (%)
120
90
60
30
0
0 1 2 3 4 5 6 7 15
Days

Supplementary Fig. 7 The optimized CD34/LNP^{DP} formulation exhibited further enhancement in transfection efficiency within CD34^{+} K562 cells.

(a) Representative flow cytometry plots showing the mRNA delivery efficiency by LNP^{DP}, IgG/LNP^{DP} or CD34/LNP^{DP} after co-incubation periods of 24, 48 and 72 h with CD34^{+} K562 cells. A concentration of 500 ng/mL LNPs was utilized.

(b) Quantitative analysis of the transfection efficiency (% mCherry^{+} cells) across distinct LNP^{DP} formulations. Data are presented as mean ± s.d. (n = 3 biologically independent samples). Statistical significance was analyzed using one-way ANOVA with Tukey's multiple comparisons test. NS, not significant.

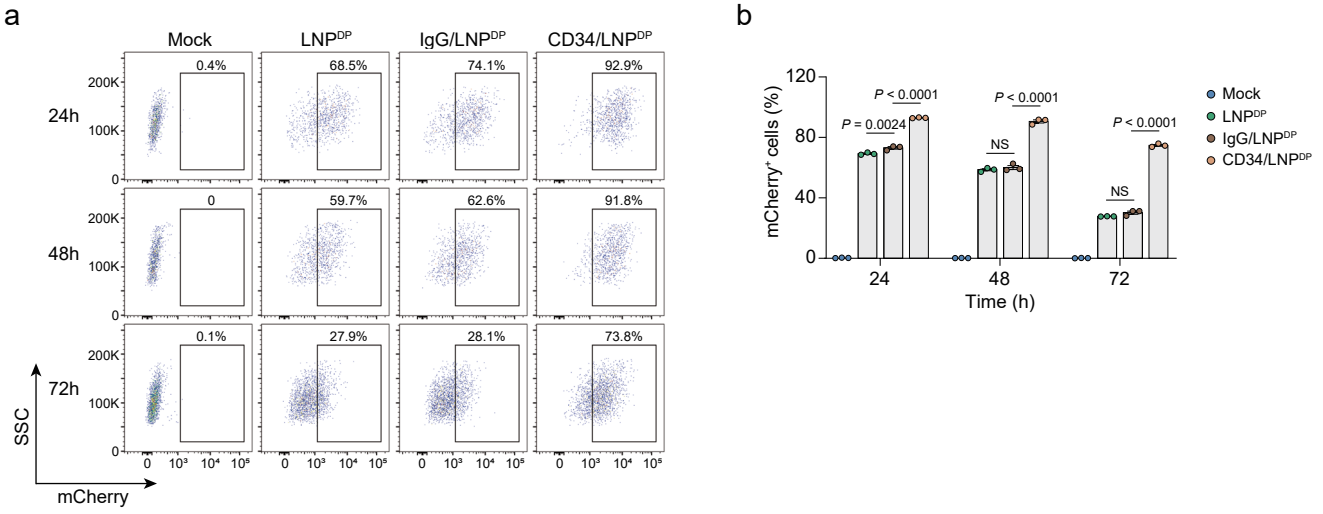
a
Mock
LNP^DP
IgG/LNP^DP
CD34/LNP^DP
24h
48h
72h
0.4%
68.5%
74.1%
92.9%
0
59.7%
62.6%
91.8%
0.1%
27.9%
28.1%
73.8%
200K
100K
0
SSC
mCherry
b
mCherry+ cells (%)
120
80
40
0
P < 0.0001
P = 0.0024
P < 0.0001
NS
P < 0.0001
NS
24
48
72
Time (h)
Mock
LNP^DP
IgG/LNP^DP
CD34/LNP^DP

Supplementary Fig. 8 Evaluation of the transfection efficiency mediated by IgG/LNPs or CD34/LNPs in WT K562 cells.

(a) Representative flow cytometry plots showing mRNA delivery efficiency in WT K562 cells following treatment with IgG/LNPs or CD34/LNPs formulated with DC18-PEG_{2k} or DC16-PEG_{2k} at indicated doses.

(b) Quantitative analysis of transfection efficiency (% $mCherry^+$ cells) across distinct LNP formulations. Data are presented as mean ± s.d. (n = 3 biologically independent samples). Statistical significance was analyzed using two-way ANOVA with Šídák's multiple comparisons test.

a

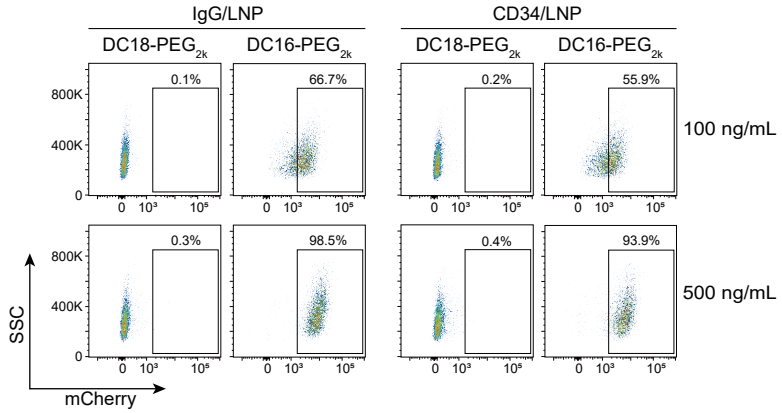
IgG/LNP
CD34/LNP
DC18-PEG2k
DC16-PEG2k
DC18-PEG2k
DC16-PEG2k
0.1%
66.7%
0.2%
55.9%
100 ng/mL
0.3%
98.5%
0.4%
93.9%
500 ng/mL
800K
400K
0
SSC
mCherry
0
10³
10⁵

b

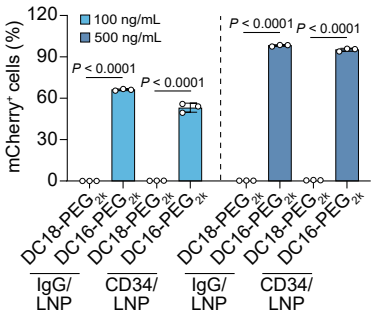
100 ng/mL
500 ng/mL
mCherry⁺ cells (%)
120
90
60
30
0
P < 0.0001
P < 0.0001
P < 0.0001
P < 0.0001
DC18-PEG2k
DC16-PEG2k
DC18-PEG2k
DC16-PEG2k
DC18-PEG2k
DC16-PEG2k
DC18-PEG2k
DC16-PEG2k
IgG/ LNP
CD34/ LNP
IgG/ LNP
CD34/ LNP

Supplementary Fig. 9 Size distribution of LNPs and estimation of LNP number per cell utilized in transfection of CD34⁺ K562 cells.

(a-c) Nanoparticle tracking analysis (NTA) of LNP^{DP} **(a)**, IgG/LNP^{DP} **(b)**, and $CD34/LNP^{DP}$ **(c)** formulations at a concentration of 2 μg/mL.

(d) Quantification of LNP concentration (nanoparticles per mL) for each LNP^{DP} formulation.

(e) Calculated average nanoparticles per cell, derived from NTA-measured particle concentrations and a cell seeding density of 5×10^5 cells/mL. Data are presented as mean ± s.d. (n = 3 biologically independent samples).

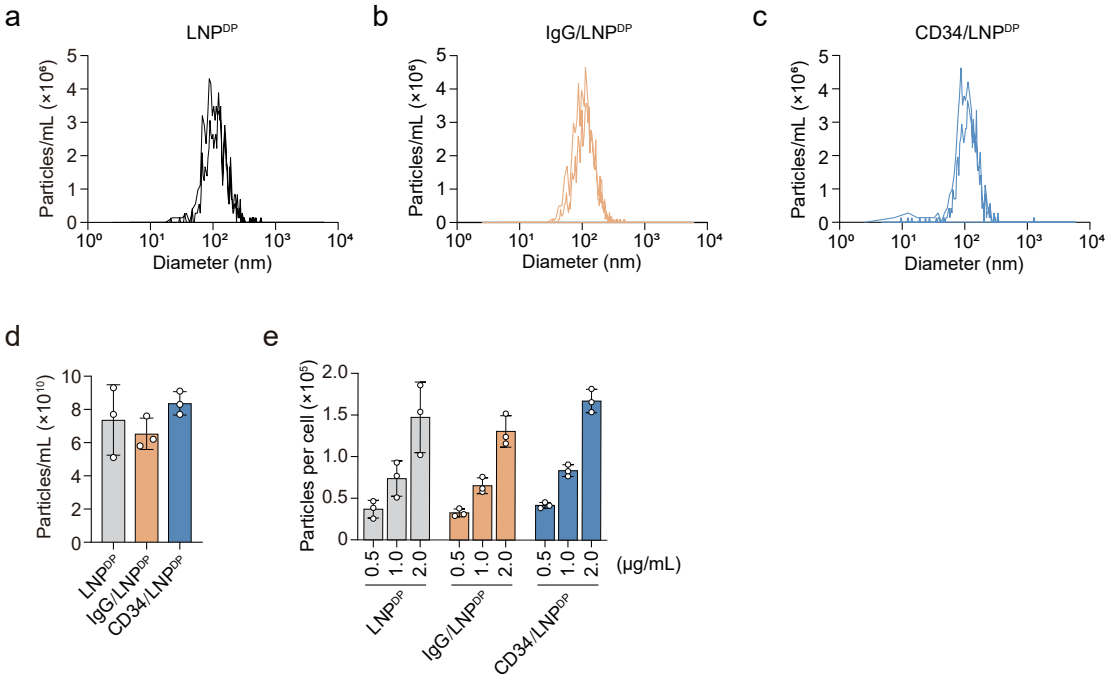
a
LNPDP
Particles/mL (×10⁶)
Diameter (nm)
b
IgG/LNPDP
Particles/mL (×10⁶)
Diameter (nm)
c
CD34/LNPDP
Particles/mL (×10⁶)
Diameter (nm)
d
Particles/mL (×10¹⁰)
LNPDP
IgG/LNPDP
CD34/LNPDP
e
Particles per cell (×10⁵)
0.5
1.0
2.0
(μg/mL)
LNPDP
IgG/LNPDP
CD34/LNPDP

Supplementary Fig. 10 Dynamics of % mCherry^{+} cells within CD34^{+} K562 cells following CD34/LNP^{DP}-mCherry transfection.

(a) Representative flow cytometry plots showing the percentage of mCherry^{+} cells at the indicated time points (0-120 hours) following treatment with 500 ng/mL CD34/LNP^{DP}-mCherry.

(b) Quantification of the percentage of mCherry^{+} cells over time. Data are represented as mean ± s.d. (n = 3 biologically independent samples).

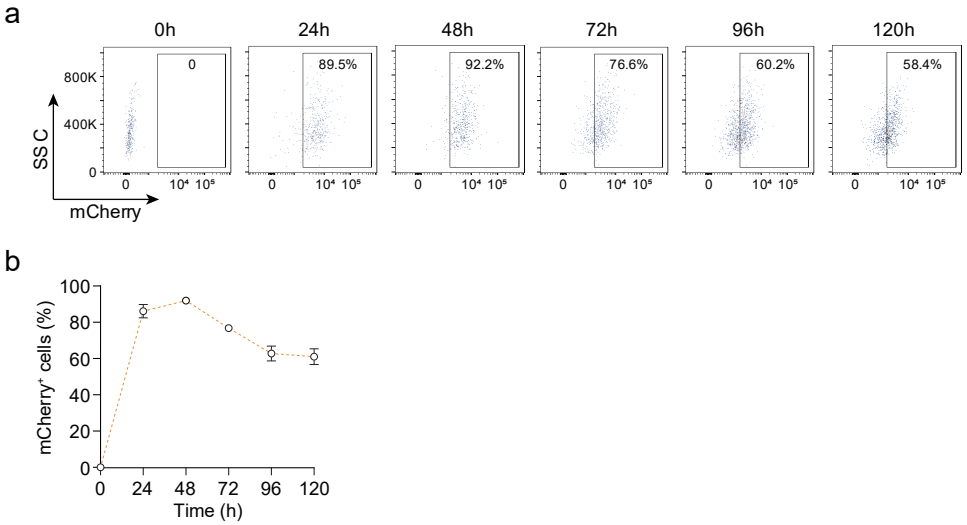
a
0h
24h
48h
72h
96h
120h
0
89.5%
92.2%
76.6%
60.2%
58.4%
800K
400K
0
SS C
mCherry
0
10⁴ 10⁵
b
mCherry⁺ cells (%)
100
80
60
40
20
0
0 24 48 72 96 120
Time (h)

Supplementary Fig. 11 CFU assay of $CD34^+$ HSPCs treated with various LNP^{DP} formulations at a concentration of 4 μg/mL for 24 hours.

Colonies were imaged on day 14 of differentiation. Scale bar, 100 μm.

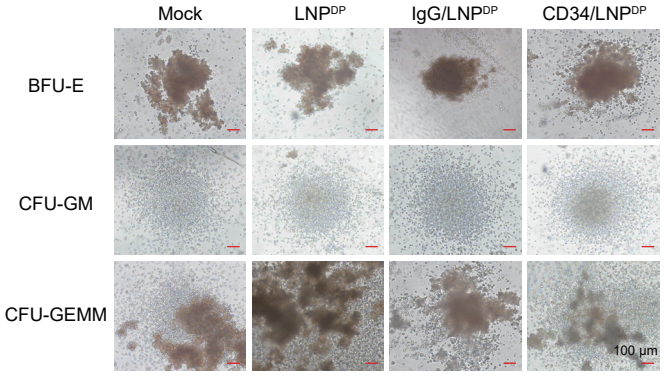
Mock
LNPDP
IgG/LNPDP
CD34/LNPDP
BFU-E
CFU-GM
CFU-GEMM
100 μm

Supplementary Fig. 12 Proliferation and transcriptomic profiling of CD34$^+$ HSPCs treated with various LNP formulations at equivalent transfection efficiency.

(a) Equivalent mCherry mRNA transfection efficiency in CD34$^+$ HSPCs mediated by LNP^{DP} and IgG/LNP^{DP} at a high concentration of 2 μg/mL, or by CD34/LNP^{DP} at a low concentration of 0.5 μg/mL.

(b) Proliferation curves of CD34$^+$ HSPCs over time following treatment with various LNP^{DP} formulations at equivalent mCherry mRNA transfection efficiency (related to panel **a**).

(c) PCA of transcriptomic profiles of CD34$^+$ HSPCs following treatment with various LNP^{DP} formulations at equivalent mCherry mRNA transfection efficiency (related to panel **a**).

(d) Heatmap of normalized expression values for selected genes across treatment groups.

Data are represented as mean ± s.d. (n = 3 biologically independent samples).

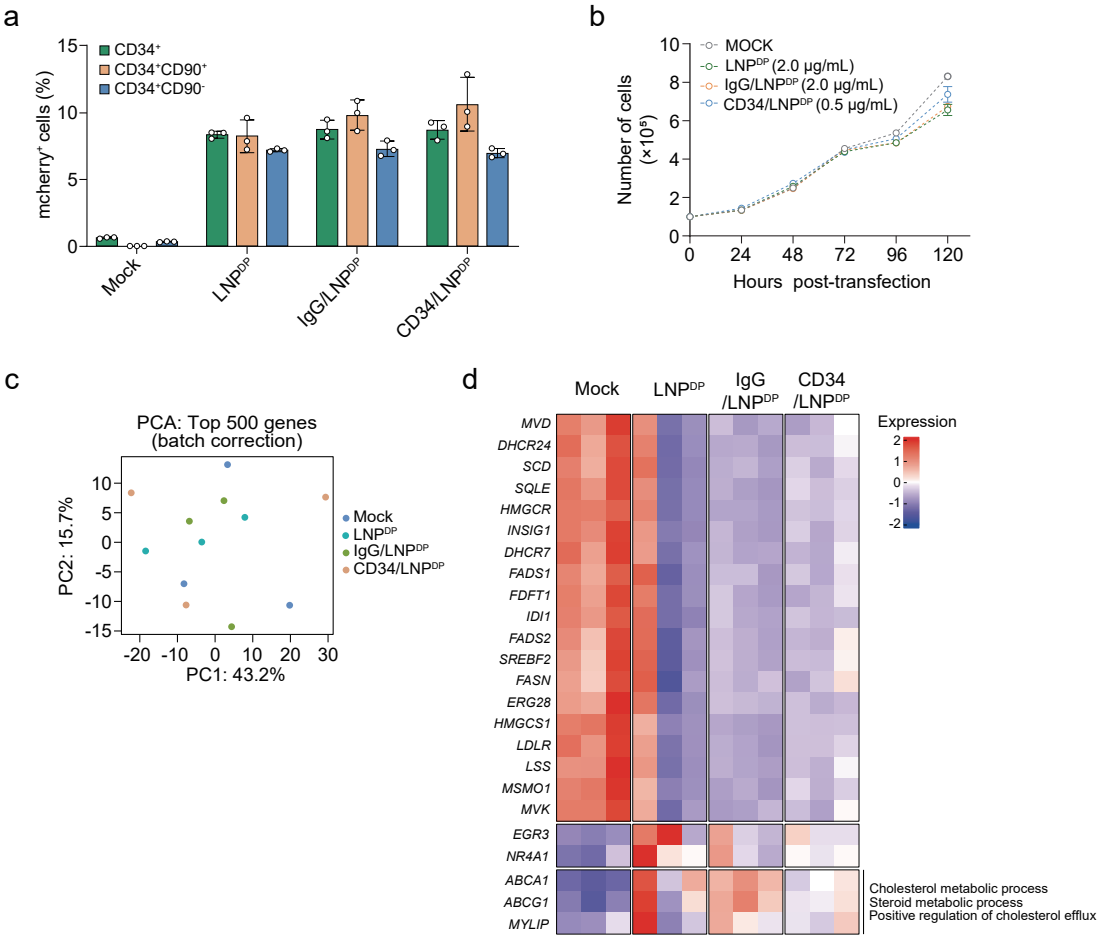
a
mcherry+ cells (%)
CD34+
CD34+CD90+
CD34+CD90-
Mock
LNPDP
IgG/LNPDP
CD34/LNPDP
b
Number of cells (×10⁵)
MOCK
LNPDP (2.0 μg/mL)
IgG/LNPDP (2.0 μg/mL)
CD34/LNPDP (0.5 μg/mL)
Hours post-transfection
c
PCA: Top 500 genes (batch correction)
PC2: 15.7%
PC1: 43.2%
Mock
LNPDP
IgG/LNPDP
CD34/LNPDP
d
Mock
LNPDP
IgG /LNPDP
CD34 /LNPDP
Expression
MVD
DHCR24
SCD
SQLE
HMGCR
INSIG1
DHCR7
FADS1
FDFT1
IDI1
FADS2
SREBF2
FASN
ERG28
HMGCS1
LDLR
LSS
MSMO1
MVK
EGR3
NR4A1
ABCA1
ABCG1
MYLIP
Cholesterol metabolic process
Steroid metabolic process
Positive regulation of cholesterol efflux

Supplementary Fig. 13 Flow cytometric gating strategies for *ex vivo* cultured CD34$^+$ HSPCs and bone marrow samples from NOG immunodeficient mice engrafted with CD34$^+$ HSPCs.

(a) Gating strategy to quantify B2M$^-$ cells within total CD34$^+$ HSPCs, CD34$^+$CD90$^+$ and CD34$^+$CD90$^-$ subsets following *ex vivo B2M* editing.

(b) Flow cytometric gating strategy to identify distinct human hematopoietic cell subsets within the bone marrow of humanized NOG mice. *B2M*-edited CD34$^+$ HSPCs were transplanted into NOG mice, and bone marrow samples were collected for flow cytometry analysis after 12 weeks. Human cells: hCD45$^+$mCD45$^-$; mouse cells: hCD45$^-$ mCD45$^+$; B cells: hCD45$^+$CD19$^+$; myeloid cells: hCD45$^+$CD33$^+$; HSPCs: hCD45$^+$CD19$^-$ CD33$^-$CD34$^+$CD90$^+$.

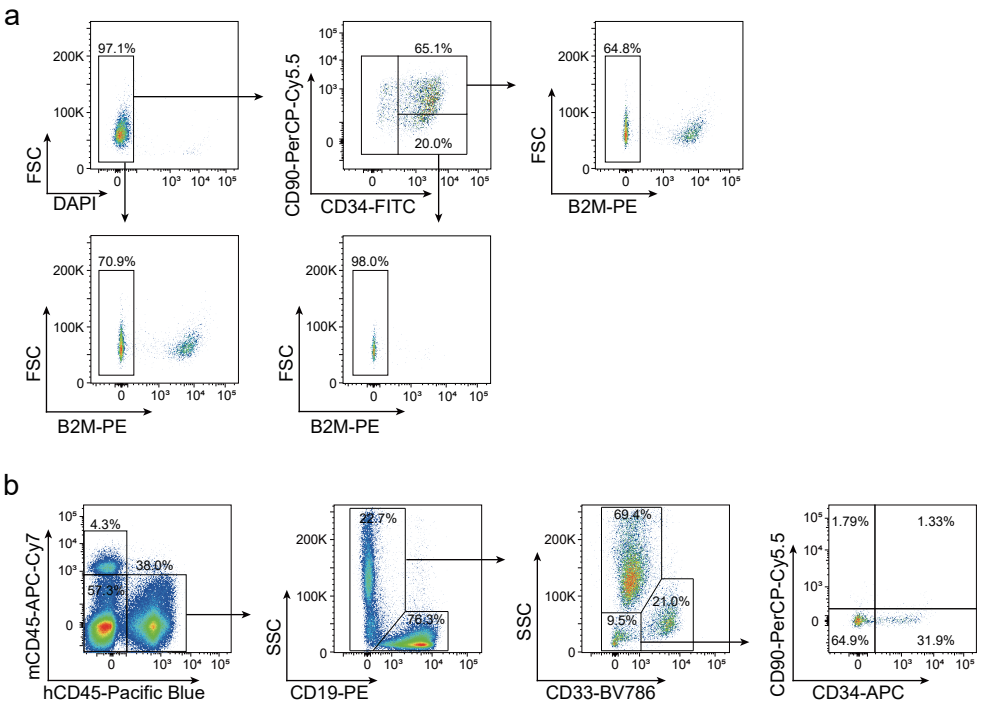
a
97.1%
FSC
DAPI
65.1%
20.0%
CD90-PerCP-Cy5.5
CD34-FITC
64.8%
FSC
B2M-PE
70.9%
FSC
B2M-PE
98.0%
FSC
B2M-PE
b
4.3%
38.0%
57.3%
mCD45-APC-Cy7
hCD45-Pacific Blue
22.7%
78.3%
SSC
CD19-PE
69.4%
21.0%
9.5%
SSC
CD33-BV786
1.79%
1.33%
64.9%
31.9%
CD90-PerCP-Cy5.5
CD34-APC

Supplementary Fig. 14 CFU assay of *B2M*-edited CD34$^+$ HSPCs mediated by CD34/LNP^{DP}.

Colonies were imaged on day 14 of differentiation. Scale bar, 100 μm.

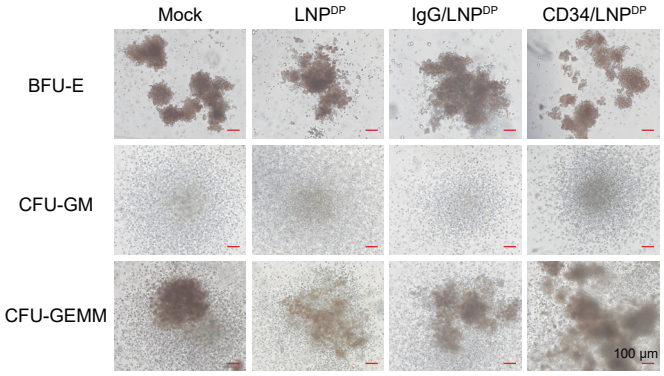
Mock
LNP^{DP}
IgG/LNP^{DP}
CD34/LNP^{DP}
BFU-E
CFU-GM
CFU-GEMM
100 μm

Supplementary Fig. 15 Profiling of erythroid differentiation and *BCL11A* editing in CD34/LNP^{DP}-treated HSPCs.

(a-b) Representative flow cytometry profiles illustrating the cellular compositions in erythroid cultures after 11- and 15-day *ex vivo* differentiation indicated by the surface marker CD71 and CD235a.

(c) Quantification of the percentage of CD71^{+}CD235a^{+} cells in erythroid cultures after 11- and 15-day *ex vivo* differentiation.

(d) ABE8e-mediated editing efficiency at the *BCL11A* core enhancer in HSPCs delivered by CD34/LNP^{DP} as determined by Sanger sequencing.

Data are represented as mean ± s.d. (n = 3 biologically independent samples). Statistical significance was analyzed using one-way ANOVA with Tukey's multiple comparisons test. NS, not significant.

Cellular composition analysis of *ex vivo* erythroid differentiation

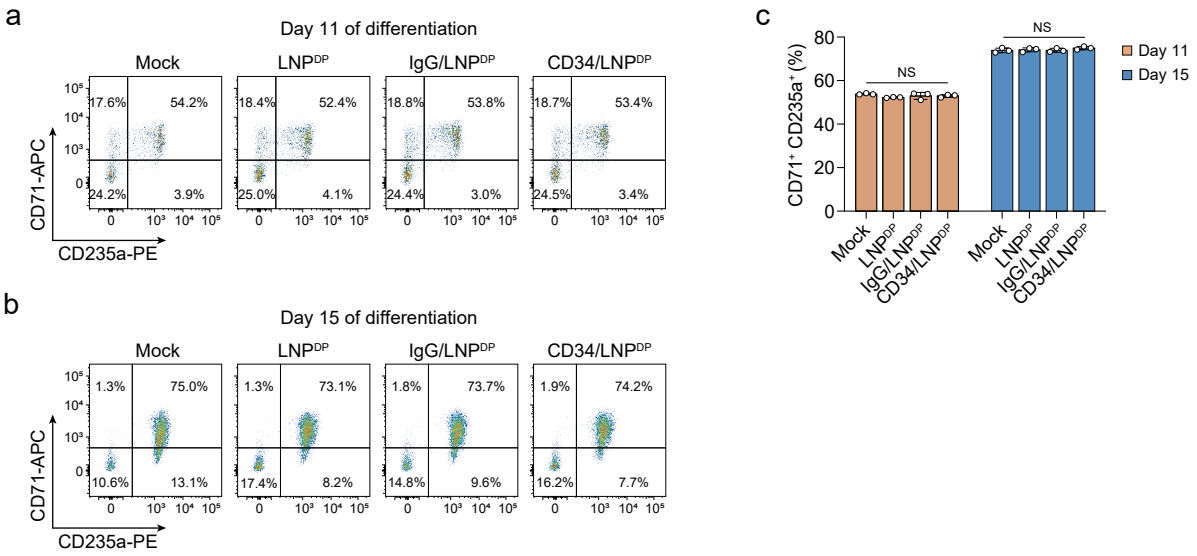

ABE8e-mediated editing efficiency at the *BCL11A* core enhancer in HSPCs delivered by CD34/LNP^{DP}

d

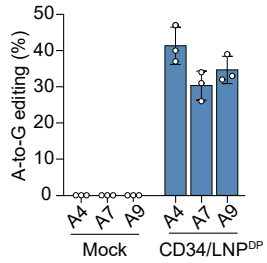

Supplementary Fig. 16 Representative gating strategy for the analysis of StayGold$^+$ populations in the bone marrow of humanized mice.

(a) Flow cytometric gating strategy to identify distinct human hematopoietic cell subsets within the bone marrow of humanized mice. Human cells: hCD45$^+$mCD45$^-$; mouse cells: hCD45$^-$mCD45$^+$; B cells: hCD45$^+$CD19$^+$; myeloid cells: hCD45$^+$CD33$^+$; HSPCs: hCD45$^+$CD19$^-$CD33$^-$CD34$^+$.

(b) The human cell chimerism level defined as hCD45$^+$/(hCD45$^+$ + mCD45$^+$), was assessed by flow cytometry. Data are represented as mean ± s.d. (n = 3 biologically independent samples). Statistical significance was analyzed using one-way ANOVA with Tukey's multiple comparisons test. NS, not significant.

(c) Quantitative assessment of StayGold$^+$ cell percentages across subpopulations of bone marrow from humanized mice.

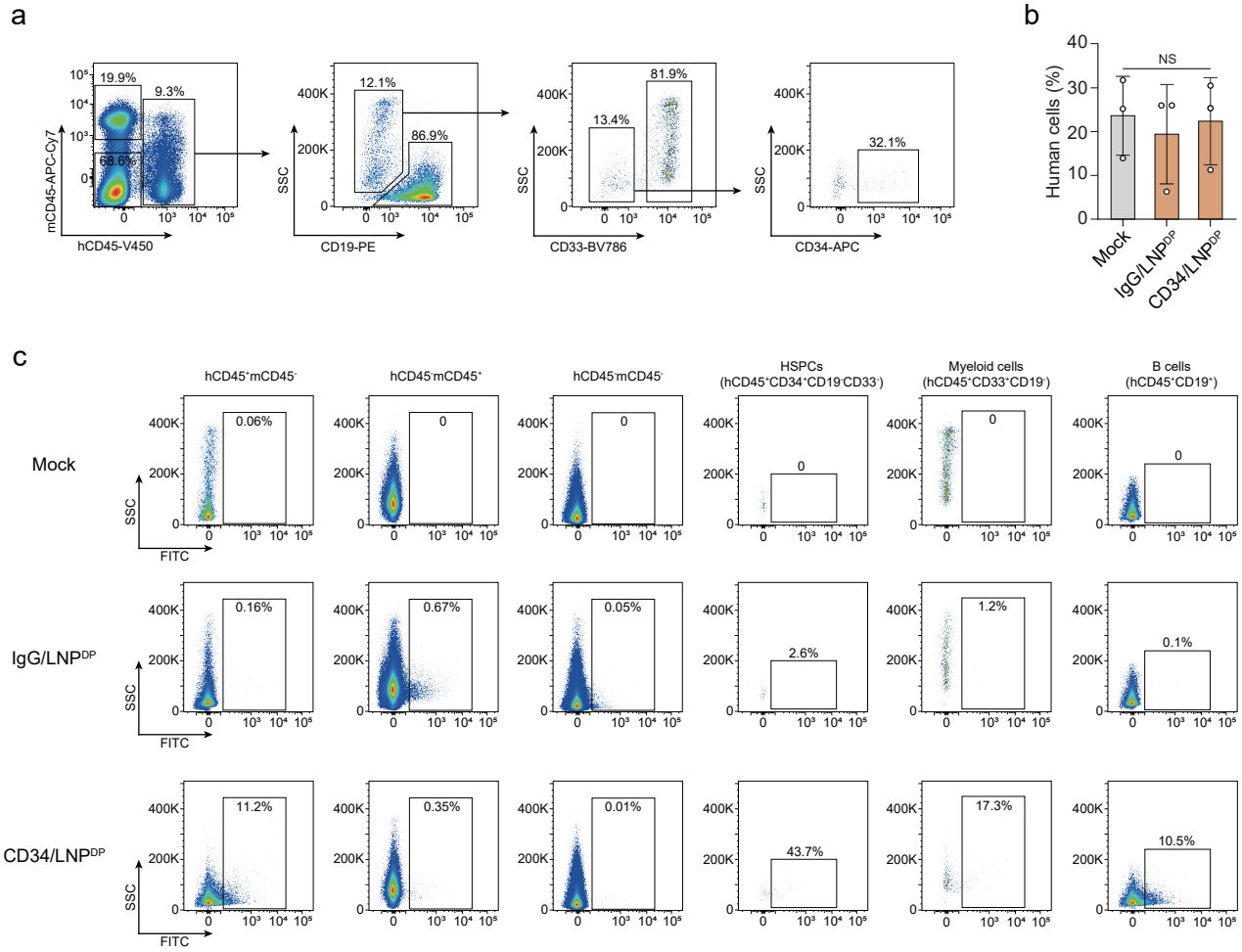
a
19.9%
9.3%
68.6%
mCD45-APC-Cy7
hCD45-V450
12.1%
86.9%
SSC
CD19-PE
81.9%
13.4%
CD33-BV786
32.1%
CD34-APC
b
Human cells (%)
NS
Mock
IgG/LNP^DP
CD34/LNP^DP
c
hCD45+mCD45-
hCD45-mCD45+
hCD45-mCD45-
HSPCs (hCD45+CD34+CD19-CD33-)
Myeloid cells (hCD45+CD33+CD19-)
B cells (hCD45+CD19+)
Mock
IgG/LNP^DP
CD34/LNP^DP
SSC
FITC
0.06%
0
0
0
0
0
0.16%
0.67%
0.05%
2.6%
1.2%
0.1%
11.2%
0.35%
0.01%
43.7%
17.3%
10.5%

Supplementary Fig. 17 *In vivo* off-target editing analysis of LNP^{DP} formulations using a conserved sgRNA and miR-122- SpCas9 mRNA.

(a) Human-mouse conserved sgRNA sequence used for *in vivo* off-target analysis. A schematic showing the sgRNA-targeting site (blue) and PAM sequence (orange). *BCL11A*-homo, human-mouse homologous region of *BCL11A*.

(b) *In vivo* editing efficiency in humanized NOG mice of LNP^{DP} or CD34/LNP^{DP} -encapsulated miR-122- SpCas9 mRNA/sg*BCL11A*-homo delivered via intrafemoral (IF) or intravenous (IV) injection, as determined by Sanger sequencing. Data are represented as mean ± s.d. (n = 3 biologically independent samples). Statistical significance was analyzed using one-way ANOVA with Tukey's multiple comparisons test.

a

BCL11A (a homologous genomic region shared between the *Homo sapiens* and *Mus musculus* genomes)

···CTTTAAGATGCCATTTTCGACTGGCCAGGCCAGAGTAGAGAGGGCAGTTGCTGAAGCGCA···

sg*BCL11A*-homo

b

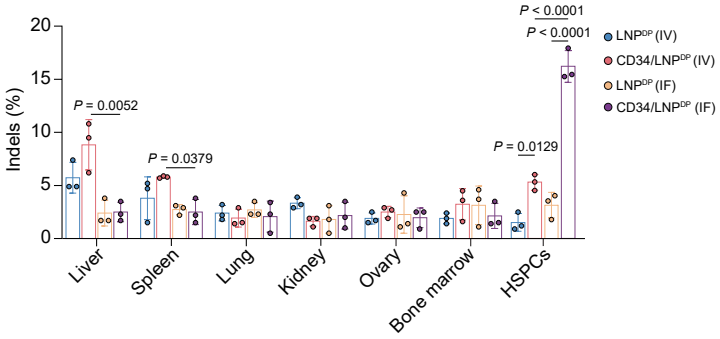

Supplementary Fig. 18 Assessment of bone marrow inflammatory response and architecture integrity following intrafemoral delivery of CD34/LNP^{DP} in mice.

(a-e) Inflammatory cytokine dynamics in the bone marrow microenvironment of humanized NOG mice after bilateral intrafemoral administration of LNP^{DP} or CD34/LNP^{DP} formulations encapsulating luciferase-encoding mRNA at 1 mg mRNA/kg. Concentrations of IL-1β **(a)**, IL-6 **(b)**, IL-10 **(c)**, TNF-α **(d)** and IFN-γ **(e)** were quantified in the bone marrow aspirate supernatants collected at 24 h and 48 h post-administration. Data represents mean ± s.d. (n = 4 mice for mock and n = 5 mice for treated group). Statistical significance was analyzed using one-way ANOVA with Tukey's multiple comparisons test.

(f) Representative hematoxylin and eosin staining of serial sections from the injected and contralateral non-injected femurs of C57BL/6J mice, harvested at 24 h and 1 week post-injection. LNP^{DP}-Luc or PBS vehicles were administered into the left distal femur. Scale bar, 50 μm.

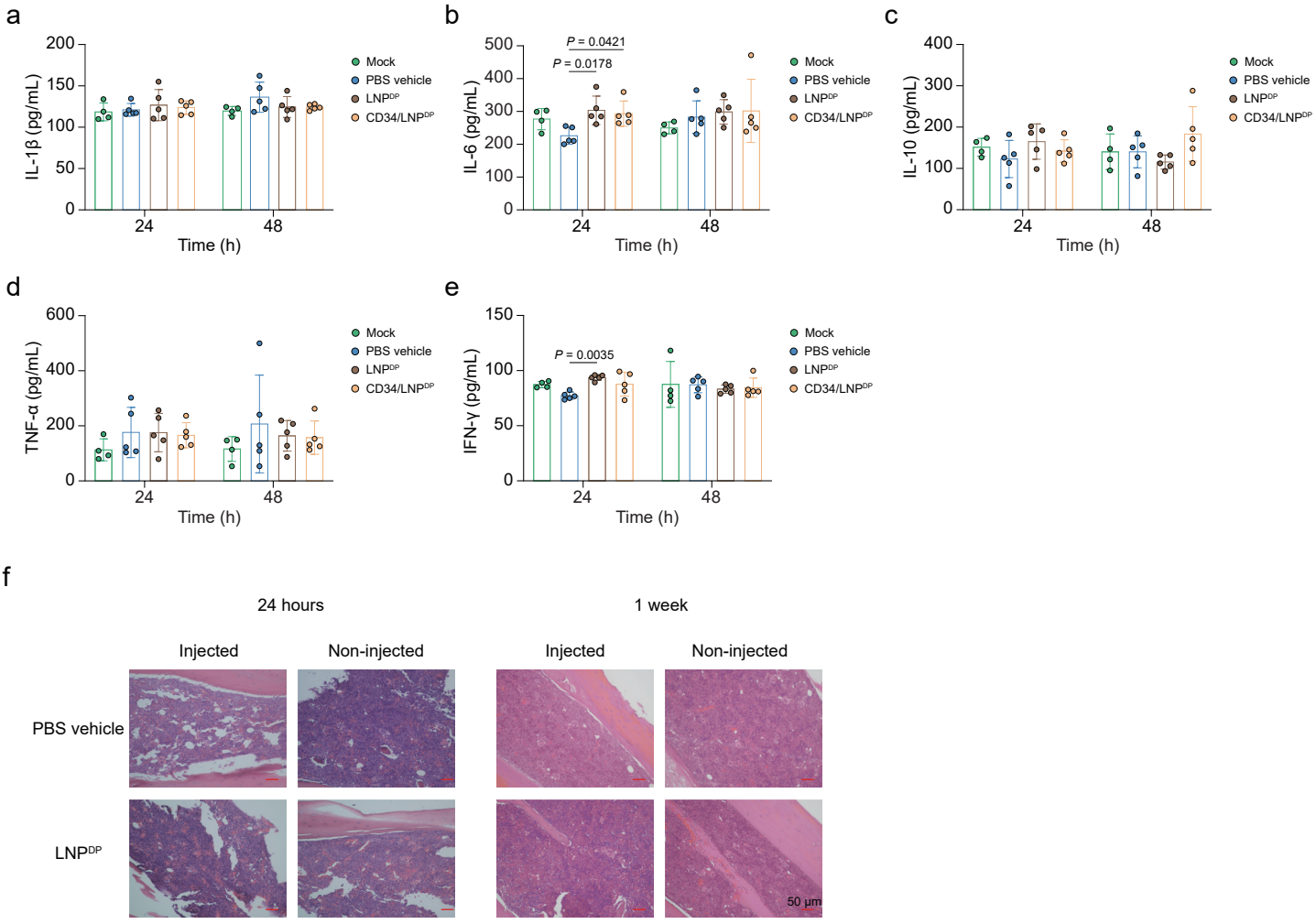
a
IL-1β (pg/mL)
200
150
100
50
0
24
48
Time (h)
Mock
PBS vehicle
LNPDP
CD34/LNPDP
b
IL-6 (pg/mL)
P = 0.0421
P = 0.0178
500
400
300
200
100
0
24
48
Time (h)
Mock
PBS vehicle
LNPDP
CD34/LNPDP
c
IL-10 (pg/mL)
400
300
200
100
0
24
48
Time (h)
Mock
PBS vehicle
LNPDP
CD34/LNPDP
d
TNF-α (pg/mL)
600
400
200
0
24
48
Time (h)
Mock
PBS vehicle
LNPDP
CD34/LNPDP
e
IFN-γ (pg/mL)
P = 0.0035
150
100
50
0
24
48
Time (h)
Mock
PBS vehicle
LNPDP
CD34/LNPDP

f
24 hours
1 week
Injected
Non-injected
Injected
Non-injected
PBS vehicle
LNPDP
50 μm

Supplementary Tables

Supplementary Table 1. Primers for plasmid construction.

Name	Sequence (5’ - 3’)
CD34-CDS-fwd	CTCCGACAGACTGAGTCGGACCGGTGCCACCATGCTGGTCCGCAGGGG
CD34-CDS-rev	CAGAGAGAAGTTTGTTGCGCCGGATCCCAATTCGGTATCAGCCACCACGTG

Supplementary Table 2. 5’ and 3’ UTR sequences for mRNA constructs.

	Sequence (5’ - 3’)
5’ UTR	AACUAGUAUUCUUCUGGUCCCCACAGACUCAGAGAGAACCCGCCACC
3’ UTR	CUGGUACUGCAUGCACGCAAUGCUAGCUGCCCCUUUCCCGUCCUGGGUACCCCGAGUCUCCCCCGACCUCGGGUCCCAGGUAUGCUCCCACCUCCACCUGCCCCACUCACCACCUCUGCUAGUUCCAGACACCUCCCAAGCACGCAGCAAUGCAGCUCAAAACGCUUAGCCUAGCCACACCCCCACGGGAAACAGCAGUGAUUAACCUUUAGCAAUAAACGAAAGUUUAACUAAGCUAUACUAACCCCAGGGUUGGUCAAUUUCGUGCCAGCCACACC

Supplementary Table 3. Primers for Sanger sequencing.

Name	Forward primer (5’ - 3’)	Reverse primer (5’ - 3’)
Human-*BCL11A*-homo	TACACACATCAGACACCTTCTCTC	CCCTTGAGCTGCCGAGAAAC
Mouse-*BCL11A*-homo	TGTATCAGAGGCAAGGTAACCAC	GAGCTGCTGAGAAACCCAC
Human-*BCL11A*-SpCas9/ABE	ATGGACCTTGGGTGCTATTC	AATGCTGCCTCCTGGTATTT

Supplementary Table 4. Primers for targeted deep sequencing.

Name	Forward primer (5' - 3')	Reverse primer (5' - 3')
Human-*B2M*	GGTGCCTGATATAGCTTGACACC	CTTCAATGTCGGATGGATGAAACC
Human-*ELANE*5-1/2	GTCCAGCTTCCCCACCTTG	GCGTTGGATGATAGAGTCGATCC
Human-*ELANE*2	CGTGGCCCTTCATGGTGTC	ACCTCACAGACCGGGACG
Human-*BCL11A*	TAACACACCAGGGTCAATACAAC	ATCACCAAGAGAGCCTTCCG

Supplementary Table 5. Primers for RT-qPCR.

Gene	Forward primer (5' - 3')	Reverse primer (5' - 3')
Human-*BCL11A*	AATTTGCCCCAAACAGGAA	GTGGGGATTAGAGCTCCATGT
Human-*HBB*	CTGAGTGAGCTGCACTGTGA	TTGGACAGCAAGAAAGCGAG
Human-*HBG*	GTGGAAGATGCTGGAGGAGAAA	TGCCATGTGCCTTGACTTTG
Human-*Gapdh*	GAGTCAACGGATTTGGTCGT	GACAAGCTTCCCGTTCTCAG